Global motion processing: The effect of spatial scale and eccentricity

Robert F. Hess

McGill Vision Research, Department of Ophthalmology, McGill University, Quebec, Canada

Craig Aaen-Stockdale

McGill Vision Research, Department of Ophthalmology, McGill University, Quebec, Canada

Here we examine how global translational motion sensitivity varies with the spatial frequency of the elements in local motion and on the eccentricity of stimulation. Using DC-balanced, spatially narrowband elements (radial log Gabors) matched in terms of multiples above contrast threshold, we show that global translational motion sensitivity is best at mid high spatial frequencies and worst at low spatial frequencies. Furthermore, we show that the lower global motion sensitivity of the periphery is due to differences in spatial scale/contrast that can be attributed to lower reaches of the visual pathway where the local motion signal is transduced. Thus, the efficiency of the global translational motion computation that occurs in extrastriate cortical areas does not vary across the visual field. This may not be directly applicable to global radial motion because there are known visual field anisotropies.

Keywords: global motion, spatial frequency, eccentricity, second order

Citation: Hess, R. F., & Aaen-Stockdale, C. (2008). Global motion processing: The effect of spatial scale and eccentricity. *Journal of Vision, 8*(4):11, 1–11, http://journalofvision.org/8/4/11/, doi:10.1167/8.4.11.

Introduction

It is thought that extrastriate cortical mechanisms underlie global motion analysis because of the large areas over which local motion summation takes place (Burr, Morrone, & Vaina, 1998; Downing & Movshon, 1989). Cells in the middle temporal area (MT) are well suited to this task because they are thought to sum multiple, spatially localized, local motion inputs within much larger receptive fields (Burr et al., 1998; Downing & Movshon, 1989; Movshon, Adelson, Gizzi, & Newsome, 1985). Moreover, lesions to this area in monkey (Newsome & Paré, 1988) and human (Baker, Hess, & Zihl, 1991) disrupt the ability to encode the direction of global motion. There is also a strong correlation between behavioral performance and cellular responses in this area (Britten, Shadlen, Newsome, & Movshon, 1992) because performance can be modified in a predictable manner by microstimulation of these cortical cells (Salzman, Murasugi, Britten, & Newsome, 1992).

The current model of global motion processing posits a two-stage process (Morrone, Burr, & Vaina, 1995). The first stage involves a contrast-dependent, local motion processing in different parts of the field at a range of different spatial scales. The second stage involves the integration of these local motion signals with early contrast saturation (Edwards, Badcock, & Nishida, 1996). The first stage has been identified with area V1 where directionally selective cells have localized receptive fields of different sizes, tuned to different ranges of spatial frequency with a strong dependence on contrast (Movshon & Newsome, 1996). Area MT has been identified with stage 2, at least for translational motion, since its cells have large receptive fields with multiple subunits and exhibit contrast independence (Fine, Anderson, Boynton, & Dobkins, 2004; Movshon et al., 1985; Rodman & Albright, 1989).

Our interest is whether sensitivity for global motion processing varies across the visual field. If it does, is this due to regional sensitivity differences in local motion processing in stage 1 of the model or regional differences in how these signals are integrated in stage 2 of the model?

This question cannot be answered without considering the spatial heterogeneity of the visual field evident in early cortical areas (Hubel & Wiesel, 1977). The visual field is heterogeneous in terms of spatial scale, with small receptive fields in the center and much larger receptive fields in the periphery (Sasaki et al., 2001). It is also heterogeneous in terms of its contrast sensitivity, having higher contrast sensitivity at any particular spatial scale in the center of the visual field (Pointer & Hess, 1989; Robson & Graham, 1981). Regardless of whether spatial scale and/or contrast is preserved at the level of global motion processing (Bex & Dakin, 2002), it will have an important influence on the local motion input to global motion detection when the sensitivity of different parts of the visual field are compared. Indeed, without this information it is not possible to obtain valid estimates of either the regional sensitivity or spatial summation properties of the underlying mechanisms.

doi: 10.1167/8.4.11 Received June 14, 2007; published April 17, 2008 ISSN 1534-7362

Spatial scale and contrast are interdependent aspects of local motion processing identified with early levels of visual processing relevant to stage 1 of the global processing model (Adelson & Bergen, 1985; van Santen & Sperling, 1985; Watson & Ahumada, 1985). Is the global motion dependence on eccentricity solely that expected from the spatial scale and contrast dependence of its local motion input (i.e., stage 1) or is there an additional loss due to global processing per se (i.e., stage 2)? When we answer this question, we also explore the related issue of how global motion processing itself depends on spatial scale.

Previously, to derive the relative low-level and high-level contributions to global motion performance, we have measured the relationship between contrast (abscissa) and global motion sensitivity (ordinate) arguing that any purely low-level contribution would shift this relationship horizontally along the contrast axis, whereas any purely global integration contribution would shift this curve vertically along the ordinate (Aaen-Stockdale, Ledgeway, & Hess, 2007a, 2007b; Hess, Hutchinson, Ledgeway, & Mansouri, 2007; Simmers, Ledgeway, Hess, & McGraw, 2003; Simmers, Ledgeway, Mansouri, Hutchinson, & Hess, 2006). Here because of the importance of spatial scale inhomogeneity considerations, we use spatial frequency narrowband elements and measure the contrast thresholds for global motion detection in central and peripheral vision, and then assess whether any central/peripheral global motion sensitivity difference can be accounted for simply by a contrast metric, in this case contrast relative to detection threshold. We do this for stimuli of different spatial frequency, speed and order (i.e., first vs. second order) (Baker & Hess, 1998).

Methods

Stimuli

Stimuli were random-dot kinematograms (RDK) made of limited lifetime, circular, isotropic, and bandpass microelements. The motion was translational left/right. Stimulus area (with the exception of the final experiment on the effect of coverage), dot number, duration, and interstimulus interval were the same for all experimental conditions. Each stimulus frame had 50 microelements, initially randomly distributed over a circular aperture area of 6-deg radius when viewed from a distance of 60 cm. Each microelement moved uniformly for 100 ms (lifetime of 6 frames) at a specified speed, typically 5.7 deg/s. When their lifetime expired, the microelements were randomly relocated inside the circular aperture. When moving outside the circular aperture, the microelements were repositioned on the opposite side of the circular aperture relative to their motion direction. The temporal phase of each element was randomized in the first frame of each motion sequence, so they appeared and disappeared randomly in time (according to a uniform distribution). The RDK motion lasted 500 ms (30 frames).

Two types of microelements were used: radial Gabors (cosine with a DC or zero frequency component) because their form is similar to the bandpass filtered dots previously used (Bex & Dakin, 2002), and radial log Gabors because they are constructed to have no DC and thus represent a better method of varying spatial scale.

Radial Gabor elements were generated according to

$$\mathrm{RadGabor}(r) = \exp(-(r^2)/(2\sigma^2)) \,.\, \cos(2\pi.r.fo), \quad (1)$$

where r is the radial position, fo is the peak frequency, and sigma defines the spatial bandwidth.

Radial log–Gabor elements were generated in the Fourier domain,

$$\mathrm{RadLogGauss}(f) = \exp((-(\log(f/fo))^2)/(2*\log(\sigma \mathrm{On}f)^2))$$
$$\text{with the constraint of } \mathrm{RadLogGauss}(0) = 0, \quad (2)$$

and then converted to the spatial domain after inverse Fourier transform:

$$\mathrm{RadLogGabor}(r) = \text{inv FFT}(\mathrm{RadLogGauss}), \quad (3)$$

where f is the radial frequency, fo is the peak frequency, and sigmaOnf defines the spatial bandwidth (1/1.5 corresponding to about 1.5 octaves). The radial log–gabors were even-symmetric in the spatial domain (i.e., bright center and dark surround); to achieve this, a zero-phase spectrum was used in the Fourier domain.

For radial Gabors and radial log Gabors, spatial bandwidth was fixed at 1 octave and peak frequency was varied (typically between 0.5 and 15 c/d).

Apparatus and calibrations

Stimuli were displayed on a Sony Trinitron monitor (E500) driven by a Bit++ device (Cambridge Research Systems, Rochester, UK), with 14-bit contrast resolution, connected to a Macintosh G4 computer running Matlab and the PsychToolbox. Display resolution was 1,024 × 768 pixels, pixel size was 0.375 mm, and frame rate was 60 Hz. The monitor was gamma-corrected in software with lookup tables using luminance measurements obtained from an Eye-One Display 2 calibration

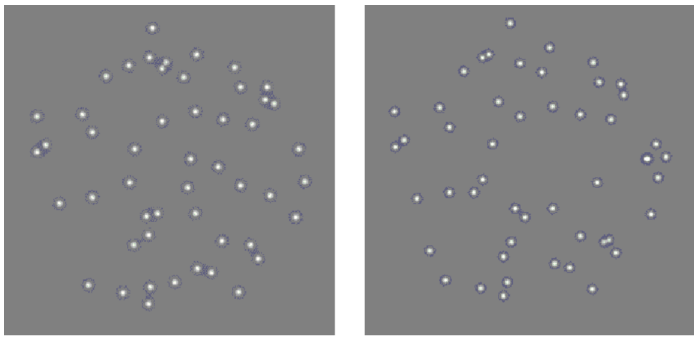

Figure 1. Example of two different stimuli used in the current investigation, radial Gabors and radial log Gabors, each with a 1-octave bandwidth.

device (Gretagmacbeth, Grand Rapids, MI). The monitor was viewed in a dimly lit room. Mean luminance of the display was 21 cd/m^2. Stimuli were viewed at 60 cm, and the display subtended 35 × 27 deg of visual angle. Stimuli were generated online, and a new RDK stimulus was generated for each presentation.

Protocol

Coherence thresholds were measured at multiples of contrast detection thresholds (typically, 3× or 5×). Contrast detection thresholds were first measured simultaneously for several element types using interleaved staircases, where subjects were required to judge the direction of homogeneous RDK stimuli presented at 70% coherence level (direction discrimination task). Coherence thresholds were then measured for an RDK stimulus of preset contrast using another staircase. In both staircase procedures, either the stimulus contrast or the coherence level was reduced after three correct responses (by 50% before the first reversal and by 25% after the first reversal) and increased by 25% after one wrong response. Each session stopped after 6 reversals, and the threshold corresponding to a criterion of about 80% correct was

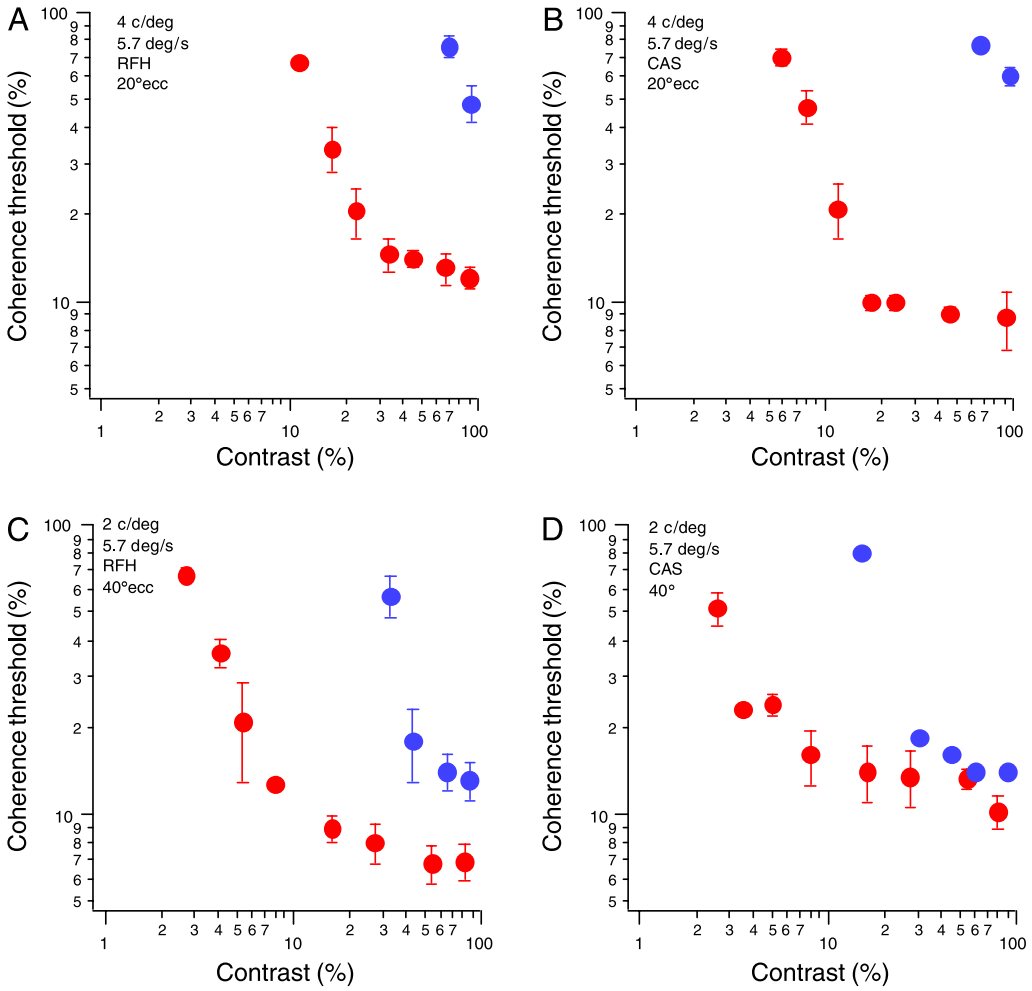

Figure 2. Global motion thresholds for two subjects as a function of element contrast for central (red) and peripheral (blue) vision. Thresholds are for RDKs composed of radial log Gabors of different spatial frequency (2 and 4 c/deg). The speed is kept constant at 5.7 deg/s.

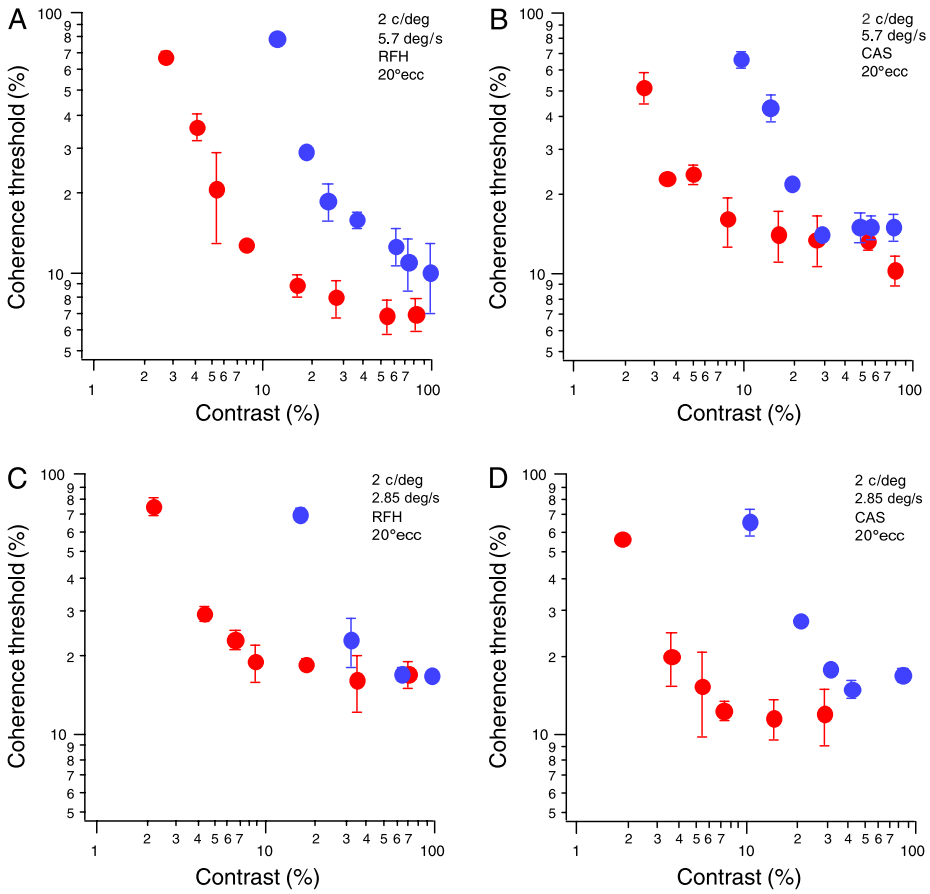

Figure 3. Global motion thresholds for two subjects as a function of element contrast for central (red) and peripheral (blue) vision. Thresholds are for RDKs composed of radial log Gabors of different speeds (5.7 deg/s and 2.85 deg/s) and constant spatial frequency (2 c/deg).

computed from the mean of the last 5 reversals. Subjects provided their responses by pressing keyboard keys associated with left and right motion.

Coherence thresholds were measured for different ranges of spatial frequency (f = [0.5–15] cpd), speed (1–30 deg/s), element type (radial gabors and radial log gabors), and order (first vs. second) of microelements.

Auditory feedback was given after each trial. A white fixation mark was briefly presented at the beginning of each trial in the center of the display. Practice trials were run before the experiments commenced. The number of trials per run for each experiment varied between 50 and 100 for each subject, and thresholds were obtained from the average of 3–4 repeats for each condition.

Results

Figure 2 shows results for two subjects for two *spatial frequencies* tested in central (red symbols) and peripheral (blue symbols) vision. Global motion thresholds (% coherence) as a function of absolute stimulus contrast (%) are shown for elements of 4 c/deg (at 0 and 20° eccentricity) and 2 c/deg (at 0 and 40° eccentricity). The error bars represent ±1 *SE*. Global motion sensitivity is better for central vision, especially at low contrasts.

Similar results are displayed in Figure 3 for two subjects for two *speeds* tested in central (red symbols) and peripheral (blue symbols) vision. Global motion thresholds at two eccentricities (0 and 20°) are shown as a function of absolute stimulus contrast. Again, global motion sensitivity is better for central vision, especially at low contrasts.

In Figure 4, contrast thresholds are shown as a function of spatial frequency for a fixed coherence level (70%) for two subjects for central and peripheral viewing. The elements are radial log Gabors. In central vision, contrast thresholds for global motion directional judgments depend on element spatial frequency, as expected, based on previous studies of local motion (Anderson & Burr, 1985). Furthermore, more contrast is required to discriminate global motion direction in peripheral vision, especially at high spatial frequencies.

Information on the contrast detection threshold for central and peripheral global motion stimuli of different spatial frequencies and speeds allows us to compare global motion coherence thresholds for stimuli of comparable contrast relative to threshold. Results in Figures 2

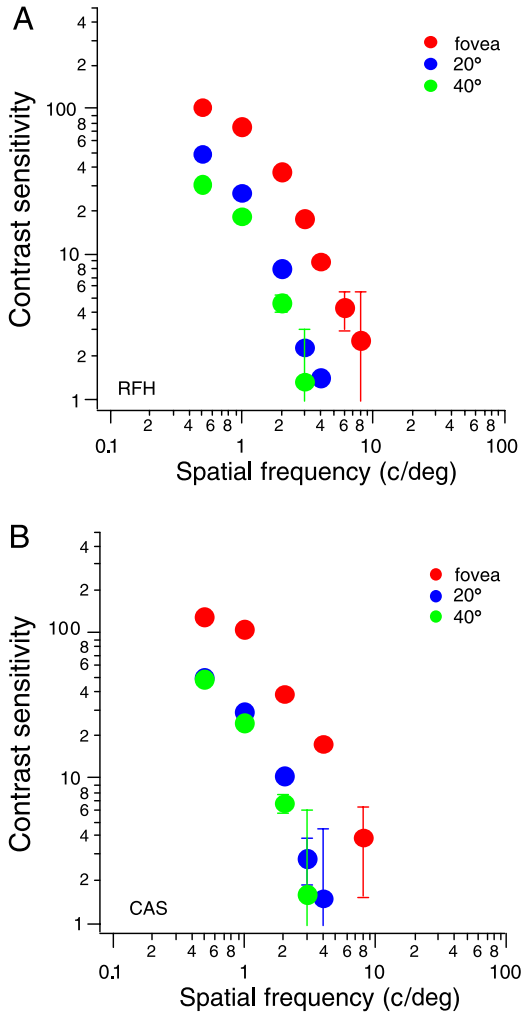

Figure 4. Contrast sensitivity for two subjects for central and peripheral (20° and 40°) direction discrimination of a field of 70% coherent RDKs composed of radial log Gabors.

and 3 are replotted in Figures 5 and 6 as contrast relative to threshold for the two subjects. It is clear now that central and peripheral sensitivity are comparable and that the central/peripheral differences seen in Figures 2 and 3 were caused by contrast threshold differences.

Another way of demonstrating this invariance of global motion thresholds across the visual field is to compare central and peripheral performance for contrast detection and global motion detection across stimulus spatial frequency for two different speeds (e.g., 1.4 deg/s and 30 deg/s) (see Figures 7 and 8). The top panels show the contrast detection thresholds and highlight the well-known difference in sensitivity of central and peripheral regions across spatial frequency for the two speeds (Kelly, 1984). The bottom two panels are coherence thresholds for central and peripheral regions for the same stimuli at the same multiple of contrast threshold. It is apparent that there is no central/peripheral difference in global motion sensitivity.

An interesting result shown in Figures 7 and 8 is the dependence of coherence threshold on stimulus spatial frequency. This has not been shown before for bandpass stimuli of this kind (having no DC) equated in terms of detectability. There appears to be a U-shaped dependence on spatial frequency similar to that for contrast detection at low speeds. This is present at both low (1.4 deg/s) and high (30 deg/s) speeds, and the low spatial frequency roll off is present for both fovea and periphery. Results shown in Figures 7 and 8 are for stimuli with contrast 3 times their contrast threshold; results displayed in Figure 9 for two subjects are for stimuli with contrast 5 times their contrast threshold. Two stimuli are compared in Figure 9, radial Gabors and radial log Gabors, each with a 1-octave bandwidth and an intermediate speed of 5.7 deg/s. The high spatial frequency roll off is not evident for either of these stimulus types, but there is a clear low spatial frequency roll off (Figures 9A and 9C) when the display area is fixed (i.e., with a radius of 6° such that element coverage varies inversely with spatial frequency but with a constant density of 0.448 micropatterns/deg^2). When the field size covaries with element spatial frequency (i.e., from a radius of 6° at 0.5 c/d to 0.375° at 8 c/d such that there was a constant coverage but a density changing from 0.448 micropattern/deg^2 to 114.9 micropatterns/deg^2), thresholds are approximately constant for both types of stimuli (Figures 9B and 9D).

For completeness we applied the same approach to the detection of second-order elements in motion. We used Gaussians of an equivalent bandwidth (i.e., 1 octave) and varied the peak modulation of a 50% contrast two-dimensional noise background. Coherence thresholds for these stimuli presented at the fovea (red symbols) and 20° peripherally (blue symbols) are displayed for two subjects in Figure 10. In Figures 10A and 10C coherence thresholds are plotted against modulation depth in percentage, whereas in Figures 10B and 10D they are plotted against modulation *relative to threshold*. Because of the insensitivity of second-order motion, the contrast range is more limited and there is less difference between foveal and peripheral coherence thresholds for these second-order stimuli. However, the same principle holds, namely, that any foveal/peripheral difference in global motion sensitivity can be accounted for by a lateral shift along the horizontal axis by an amount equivalent to the difference in modulation detection thresholds.

Discussion

An interesting spinoff of this study is the relationship between spatial scale and global motion sensitivity. It has been commonplace to use spatial frequency broadband elements in global motion tasks under the implicit assumption that at the level at which global motion

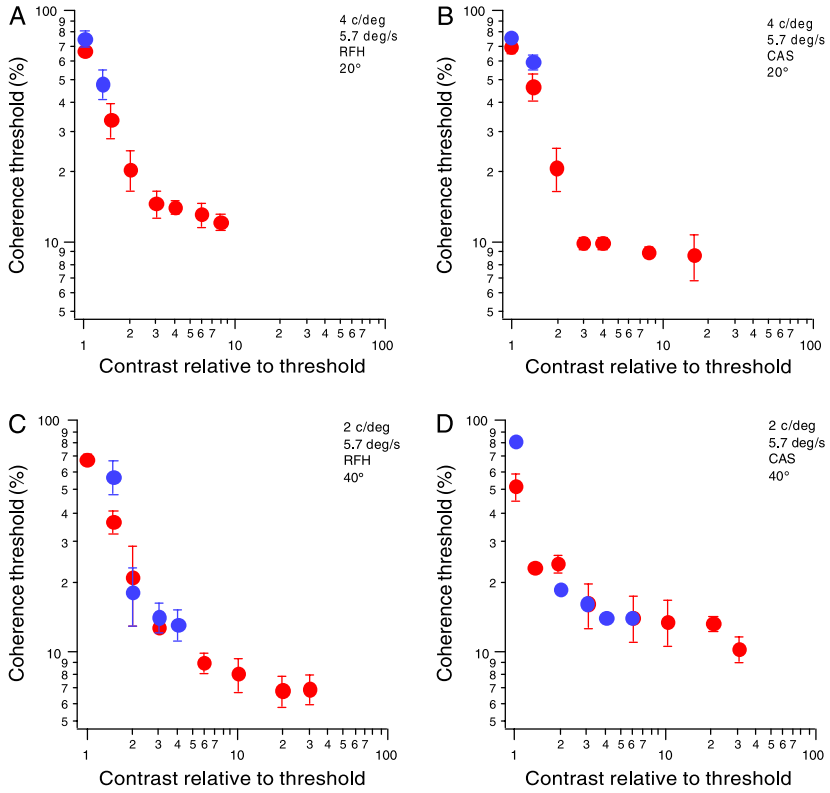

Figure 5. Results of Figure 2 replotted as contrast relative to threshold.

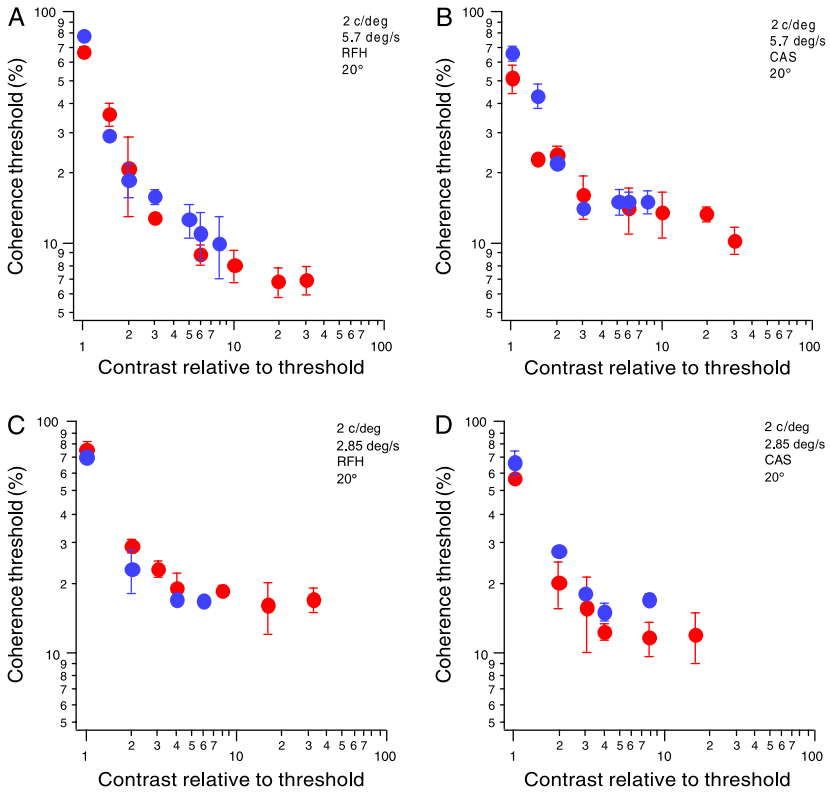

Figure 6. Results from Figure 3 replotted as contrast relative to threshold.

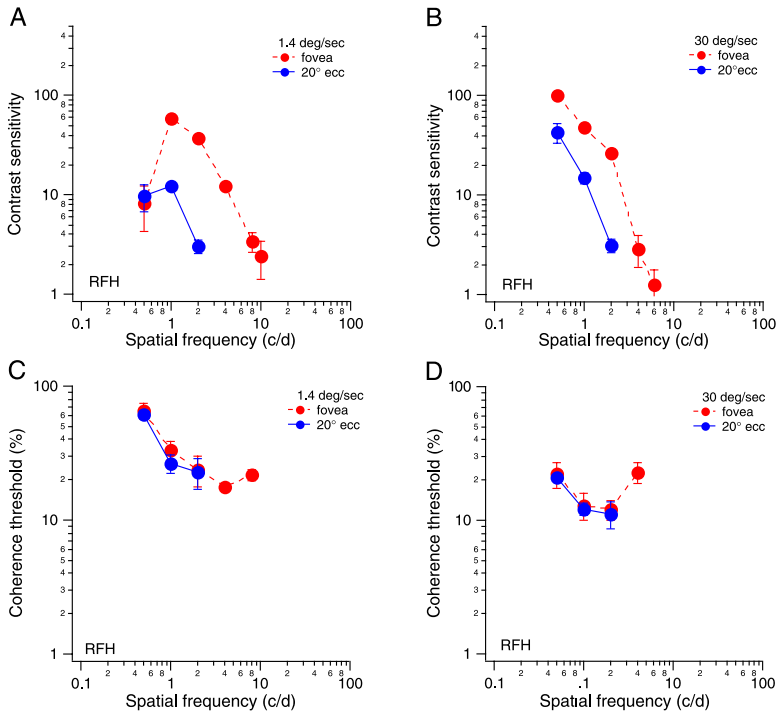

Figure 7. Comparison of subject RFH's central (red) and peripheral (blue) contrast sensitivity (top row) and coherence threshold (bottom row) across element spatial frequency for two speeds (1.4 deg/s left column and 30 deg/s right column).

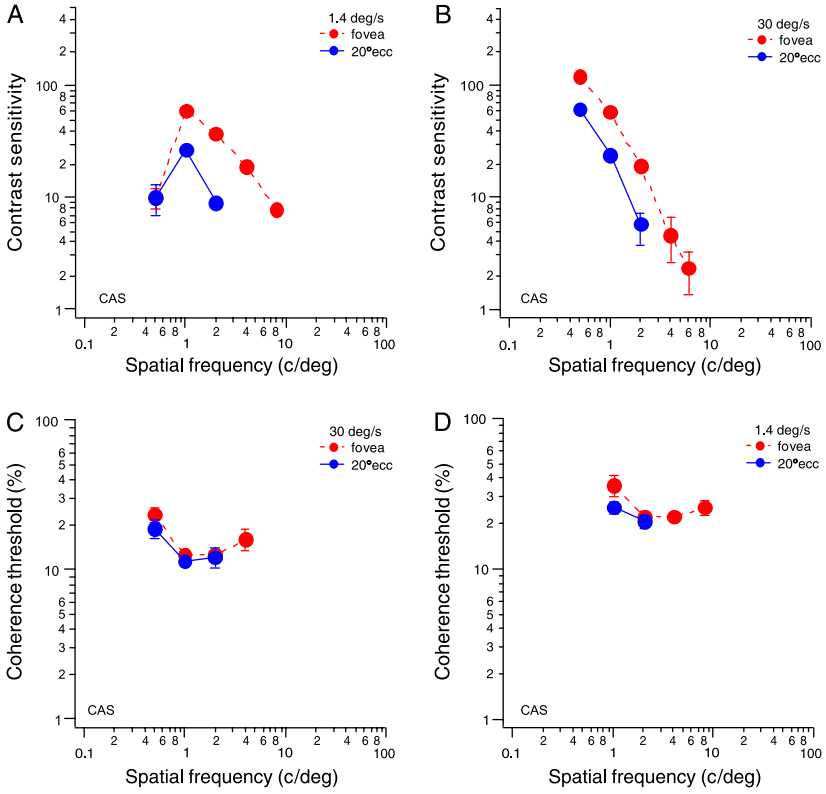

Figure 8. Comparison of subject CAS's central (red) and peripheral (blue) contrast sensitivity (top row) and coherence threshold (bottom row) across element spatial frequency for two speeds (1.4 deg/s left column and 30 deg/s right column).

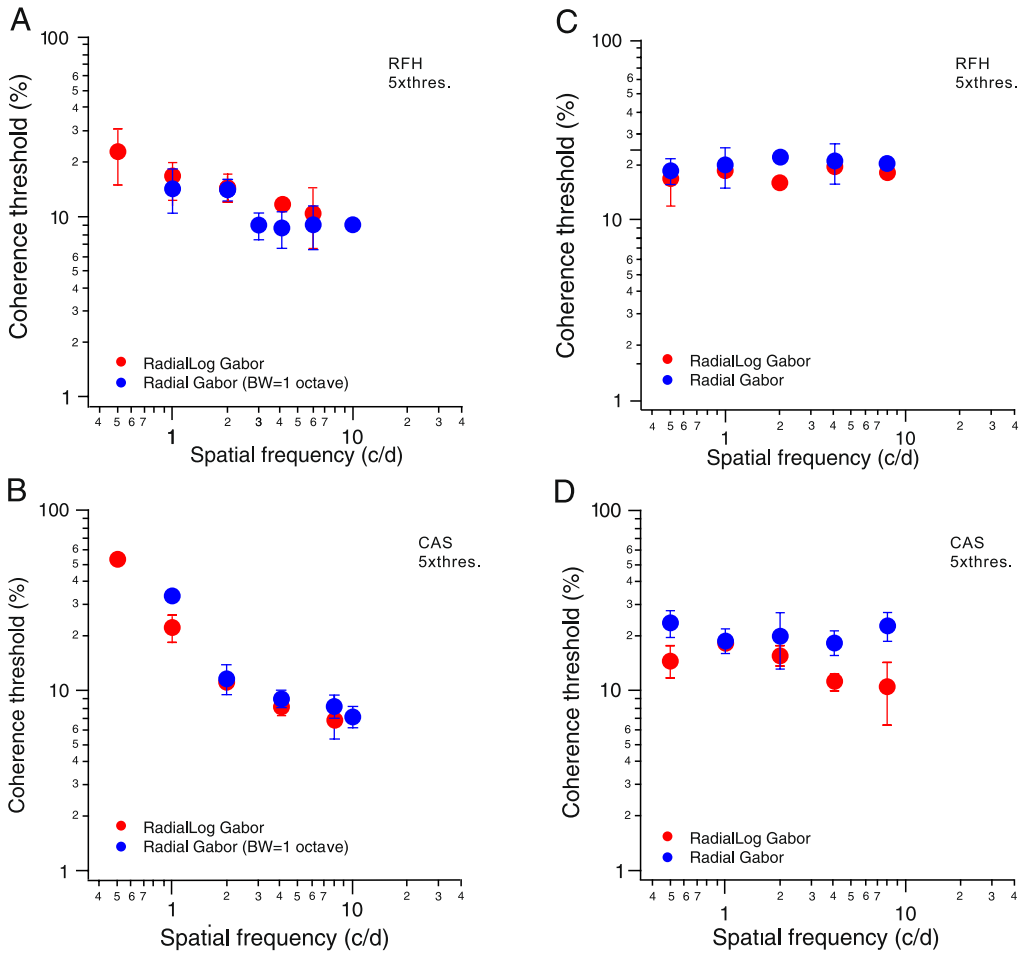

Figure 9. Coherence threshold functions (A and B) for two subjects for two stimuli (radial Gabors blue symbols and radial log Gabors red symbols), each with a 1-octave bandwidth, a constant field size (i.e., constant element density), a contrast of 5× threshold, and a speed of 5.7 deg/s. Comparable results are shown in panels C and D for radial log Gabors (red symbols) and radial Gabors (blue symbols) in which the field size covaries with spatial frequency (i.e., constant element coverage).

integration occurs, information is collapsed across scale. We show the importance of the contrast/spatial scale relationship presumably reflecting the local motion input to global motion integration. Furthermore, we show that if global motion stimuli are presented at comparable contrasts relative to threshold, there is a scale dependence per se for global motion integration. Low spatial scales exhibit slightly worse sensitivity compared to finer scales. The low spatial frequency roll off in sensitivity is robust to changes in speed (1.4 deg/s to 30 deg/s), eccentricity (0° and 20°), stimulus-type (radial Gabors and radial log Gabors), and suprathreshold contrast (×3 and ×5 times threshold) but not to changes in field size. The element density was held constant as spatial frequency was changed so that at a fixed field size the coverage covaried with spatial frequency. Restricting the lower spatial frequency elements to fall within a fixed field size may be the reason why radial Gabors and radial Log Gabors exhibit raised threshold for low spatial frequencies (see Figure 9). One implication of coverage rather than density achieving comparable sensitivity across scale is that the underlying detectors have a subunit architecture that scales with spatial frequency in the same way. In turn, this leaves open the possibility that there are separate global detectors for different spatial scales of first-order motion—a suggestion that runs contrary to the prevailing opinion (Bex & Dakin, 2002) that information is collapsed across spatial scale at the level of global motion integration. Alternatively, it could be the result of changes in the informational motion content (i.e., correspondence noise) of stimuli as spatial frequency is varied and aperture size and density are covaried. For example, it has been shown that coherence thresholds of an ideal observer improve as the aperture area increases but deteriorate as the grid location of elements gets larger (Barlow & Tripathy, 1997). The result of these two opposing effects may have resulted fortuitously in the relatively invariant response with spatial frequency

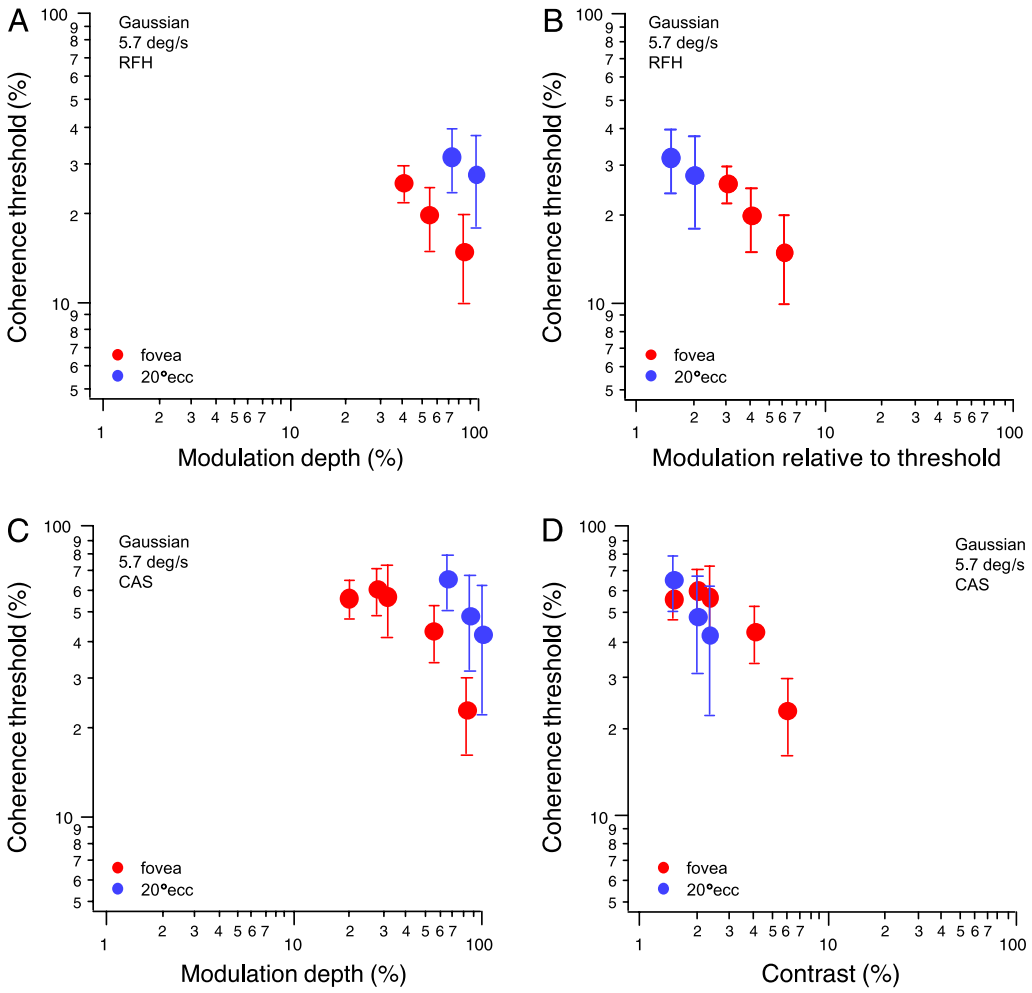

Figure 10. Global motion thresholds for two subjects as a function of element modulation depth (A and C in absolute units; B and D in units relative to detection threshold) for central (red) and 20° peripheral (blue) eccentricities for RDKs composed of second-order Gaussians with 1-octave bandwidth and a speed of 5.7 deg/s.

depicted in Figures 9B and 9D. The high spatial frequency roll off was seen only at the lower suprathreshold contrast.

The chief finding is that thresholds for direction discrimination of global motion are lower in central than in peripheral vision for a range of different spatial scales and speeds. However, central and peripheral coherence thresholds can be equated by a simple horizontal shift along the contrast axis by an amount equal to the difference in the contrast detection thresholds. This means that global motion sensitivity for stimuli of comparable suprathreshold contrast is the same across the visual field. Since the visual field is spatially inhomogeneous, the use of spatial frequency narrowband stimuli is a fundamental consideration here.

The notion that central and peripheral visual sensitivity can be brought into line by simply scaling the central stimuli has a long history. It has been shown previously that size and velocity scaling can be successful in equating central and peripheral spatiotemporal contrast sensitivity (Rovamo, Virsu, & Näsänen, 1978; Virsu, Rovamo, Laurinen, & Näsänen, 1982). This has also been extended to surface scaling for two-dimensional stimuli (Johnston, 1987). The use of contrast threshold scaling here supports this general approach. The finding that global motion performance can be equated across the visual field using solely a contrast metric suggests that all the eccentricity effects occur at a low stage of visual processing where local motion is computed and where contrast and spatial scale are important (i.e., stage 1 of the model). The larger receptive fields of cells in, for example, middle temporal area (MT) that integrate local motion information do so with equal efficiency regardless of their position in the visual field, a conclusion that is consistent with the results of Dakin, Mareschal, and Bex (2005), who used an equivalent noise approach and showed that the sole determinant of global sensitivity was number of elements in local motion. This conclusion is also consistent with the idea that any eccentricity-dependent effects seen in the responses of MT cells are simply a reflection of their V1 input (Pack, Conway, Born, & Livingstone, 2006).

The question remains as to why the sole determinant of peripheral global sensitivity should be the contrast threshold for motion direction discrimination and not, for example, perceived contrast? Perceived contrast of peripheral targets is veridical above threshold (Hess & Bradley, 1980) and would have given quite a different prediction. It is possible that perceived contrast, being a higher level attribute, might not be relevant at the low level where local motion is computed. There is, however, some evidence that local motion detection depends on contrast at least in the low-contrast range (Nakayama & Silverman, 1985) and that the relevant parameter is the contrast relative to threshold (Boulton & Hess, 1990).

A caveat: These conclusions for translational motion must be qualified in light of the known visual field motion anisotropies that have been reported for radial motion (e.g., Dumoulin, Baker & Hess, 2001; Edwards & Badcock, 1993). Factors other than local motion sensitivity in different parts of the visual field determine regional motion sensitivity for radial motion (e.g., upper vs. lower field or centripetal vs. centrifugal motion).

Acknowledgments

This work was supported by an Natural Sciences and Engineering Research Council of Canada grant (#46528-06).

Commercial relationships: none.
Corresponding author: Robert F. Hess.
Email: robert.hess@mcgill.ca.
Address: Dept. of Ophthalmology, McGill University Health Centre, Montreal, QC, H3A 1A1, Canada.

References

Aaen-Stockdale, C., Ledgeway, T., & Hess, R. F. (2007a). Second-order optic flow processing. *Vision Research, 47,* 1798–1808. [PubMed]

Aaen-Stockdale, C., Ledgeway, T., & Hess, R. F. (2007b). Second-order optic flow deficits in amblyopia. *Investigative Ophthalmology & Visual Science, 48,* 5532–5538. [PubMed]

Adelson, E. H., & Bergen, J. R. (1985). Spatiotemporal energy models for the perception of motion. *Journal of the Optical Society of America A, Optics and Image Science, 2,* 284–299. [PubMed]

Anderson, S. J., & Burr, D. C. (1985). Spatial and temporal selectivity of the human motion detection system. *Vision Research, 25,* 1147–1154. [PubMed]

Baker, C. L., Jr., & Hess, R. F. (1998). Two mechanisms underlie processing of stochastic motion stimuli. *Vision Research, 38,* 1211–1222. [PubMed]

Baker, C. L., Jr., Hess, R. F., & Zihl, J. (1991). Residual motion perception in a "motion-blind" patient, assessed with limited-lifetime random dot stimuli. *Journal of Neuroscience, 11,* 454–461. [PubMed] [Article]

Barlow, H., & Tripathy, S. P. (1997). Correspondence noise and signal pooling in the detection of coherent visual motion. *Journal of Neuroscience, 17,* 7954–7966. [PubMed] [Article]

Bex, P. J., & Dakin, S. C. (2002). Comparison of the spatial-frequency selectivity of local and global motion detectors. *Journal of the Optical Society of America A, Optics, Image Science, and Vision, 19,* 670–677. [PubMed]

Boulton, J. C., & Hess, R. F. (1990). Luminance contrast and motion detection. *Vision Research, 30,* 175–179. [PubMed]

Britten, K. H., Shadlen, M. N., Newsome, W. T., & Movshon, J. A. (1992). The analysis of visual motion: A comparison of neuronal and psychophysical performance. *Journal of Neuroscience, 12,* 4745–4765. [PubMed] [Article]

Burr, D. C., Morrone, M. C., & Vaina, L. M. (1998). Large receptive fields for optic flow detection in humans. *Vision Research, 38,* 1731–1743. [PubMed]

Dakin, S. C., Mareschal, I., & Bex, P. J. (2005). Local and global limitations on direction integration assessed using equivalent noise analysis. *Vision Research, 45,* 3027–3049. [PubMed]

Downing, C. J., & Movshon, J. A. (1989). Spatial and temporal summation in the detection of motion in stochastic random dot displays. *Investigative Ophthalmology & Vision Science, 30,* 72.

Dumoulin, S. O., Baker, C. L., Jr., & Hess, R. F. (2001). Centrifugal bias for second-order but not first-order motion. *Journal of the Optical Society of America A, Optics, Image Science, and Vision, 18,* 2179–2189. [PubMed]

Edwards, M., & Badcock, D. R. (1993). Asymmetries in the sensitivity to motion in depth: A centripetal bias. *Perception, 22*, 1013–1023. [PubMed]

Edwards, M., Badcock, D. R., & Nishida, S. (1996). Contrast sensitivity of the motion system. *Vision Research, 36,* 2411–2421. [PubMed]

Fine, I., Anderson, C. M., Boynton, G. M., & Dobkins, K. R. (2004). The invariance of directional tuning with contrast and coherence. *Vision Research, 44,* 903–913. [PubMed]

Hess, R. F., & Bradley, A. (1980). Contrast perception above threshold is only minimally impaired in human amblyopia. *Nature, 287,* 463–464. [PubMed]

Hess, R. F., Hutchinson, C. V., Ledgeway, T., & Mansouri, B. (2007). Binocular influences on global

motion processing in the human visual system. *Vision Research, 47,* 1682–1692. [PubMed]

Hubel, D. H., & Wiesel, T. N. (1977). Functional architecture of the macaque monkey visual cortex. Ferrier Lecture. *Proceedings of the Royal Society of London B: Biological Sciences, 198,* 1–59. [PubMed]

Johnston, A. (1987). Spatial scaling of central and peripheral contrast-sensitivity functions. *Journal of the Optical Society of America A, Optics and Image Science, 4,* 1583–1593. [PubMed]

Kelly, D. H. (1984). Retinal inhomogeneity. I. Spatiotemporal contrast sensitivity. *Journal of the Optical Society of America A, Optics and Image Science, 1,* 107–113. [PubMed]

Morrone, M. C., Burr, D. C., & Vaina, L. M. (1995). Two stages of visual processing for radial and circular motion. *Nature, 376,* 507–509. [PubMed]

Movshon, J. A., Adelson, E. H., Gizzi, M. S., & Newsome, W. T. (1985). The analysis of moving visual patterns. In C. Chagass, R. Gattass, & C. Gross (Eds.), *Pattern recognition mechanisms, Pontificiae academiae scientarum scripta varia* (vol. 45, pp. 117–151). Rome: Vatican Press.

Movshon, J. A., & Newsome, W. T. (1996). Visual response properties of striate cortical neurons projecting to area MT in macaque monkeys. *Journal of Neuroscience, 16,* 7733–7741. [PubMed] [Article]

Nakayama, K., & Silverman, G. H. (1985). Detection and discrimination of sinusoidal grating displacements. *Journal of the Optical Society of America A, Optics and Image Science, 2,* 267–274. [PubMed]

Newsome, W. T., & Paré, E. B. (1988). A selective impairment of motion perception following lesions of the middle temporal visual area (MT). *Journal of Neuroscience, 8,* 2201–2211. [PubMed] [Article]

Pack, C. C., Conway, B. R., Born, R. T., & Livingstone, M. S. (2006). Spatiotemporal structure of nonlinear subunits in macaque visual cortex. *Journal of Neuroscience, 26,* 893–907. [PubMed] [Article]

Pointer, J. S., & Hess, R. F. (1989). The contrast sensitivity gradient across the human visual field: With emphasis on the low spatial frequency range. *Vision Research, 29,* 1133–1151. [PubMed]

Robson, J. G., & Graham, N. (1981). Probability summation and regional variation in contrast sensitivity across the visual field. *Vision Research, 21,* 409–418. [PubMed]

Rodman, H. R., & Albright, T. D. (1989). Single-unit analysis of pattern-motion selective properties in the middle temporal visual area (MT). *Experimental Brain Research, 75,* 53–64. [PubMed]

Rovamo, J., Virsu, V., & Näsänen, R. (1978). Cortical magnification factor predicts the photopic contrast sensitivity of peripheral vision. *Nature, 271,* 54–56. [PubMed]

Salzman, C. D., Murasugi, C. M., Britten, K. H., & Newsome, W. T. (1992). Microstimulation in visual area MT: Effects on direction discrimination performance. *Journal of Neuroscience, 12,* 2331–2355. [PubMed] [Article]

Sasaki, Y., Hadjikhani, N., Fischl, B., Liu, A.K., Marrett, S., Dale, A. M., et al. (2001). Local and global attention are mapped retinotopically in human occipital cortex. *Proceedings of the National Academy of Sciences of the United States of America, 98,* 2077–2082. [PubMed] [Article]

Simmers, A. J., Ledgeway, T., Hess, R. F., & McGraw, P. V. (2003). Deficits to global motion processing in human amblyopia. *Vision Research, 43,* 729–738. [PubMed]

Simmers, A. J., Ledgeway, T., Mansouri, B., Hutchinson, C. V., & Hess, R. F. (2006). The extent of the dorsal extra-striate deficit in amblyopia. *Vision Research, 46,* 2571–2580. [PubMed]

van Santen, J. P., & Sperling, G. (1985). Elaborated Reichardt detectors. *Journal of the Optical Society of America A, Optics and Image Science, 2,* 300–321. [PubMed]

Virsu, V., Rovamo, J., Laurinen, P., & Näsänen, R. (1982). Temporal contrast sensitivity and cortical magnification. *Vision Research, 22,* 1211–1217. [PubMed]

Watson, A. B., & Ahumada, A. J., Jr. (1985). Model of human visual-motion sensing. *Journal of the Optical Society of America A, Optics and Image Science, 2,* 322–341. [PubMed]